The Structure of *meta*-Benzyne Revisited—A Close Look into *σ*-Bond Formation

Michael Winkler and Wolfram Sander*

Lehrstuhl für Organische Chemie II der Ruhr-Universität Bochum, Universitätsstr. 150, 44780 Bochum, Germany

Received: June 1, 2001; In Final Form: July 25, 2001

A detailed density fuctional theory (DFT) and ab initio quantum chemical investigation of *meta*-benzyne (**1**) is presented with a focus on the distance of the radical centers C1 and C3. Energy profiles for the cyclization of the biradical form (**1a**) to give the highly strained bicyclic anti-Bredt olefin (**1b**) are calculated employing four different functionals (B3LYP, B3PW91, BLYP, BPW91) as well as different ab initio methods (HF, MP2, CASSCF) in combination with two different basis sets (cc-pVDZ, cc-pVTZ). To judge the performance of the different methods, high-level single-point calculations (CCSD(T)/cc-pVTZ, CASPT2/cc-pVTZ, and CAS(8,8)-CISD+Q/cc-pVTZ) are carried out for a large number of structures along the cyclization coordinate. These calculations show that only one minimum energy structure exists for *meta*-benzyne and that the C1C3 separation is 205 ± 5 pm. The topology of the PES as well as the equilibrium geometry strongly depend on the level of theory applied. Hybrid DFT methods overestimate bonding between the radical centers, pure GGA methods perform significantly better, and the BLYP fuctional appears to be the most suitable one for aromatic *meta*-biradicals. Despite the large distance of the radical centers in **1,** the biradical character is low (19−32% depending on the definition of this quantity) and therefore neither **1a** nor **1b** is an appropriate representation of *meta*-benzyne. NBO population and topological analysis of the electron density distribution reveal that the best way to describe the electronic structure of this molecule is a *σ*-allylic system in which primarily the antibonding C2H7 orbital participates in the interaction of the radical lobes.

1. Introduction

Aromatic biradicals[1] have been the subject of many experimental[2−5] and computational[6−9] studies during the last years. Much effort has been spent to elucidate the structure and reactivity of *ortho*- and *para*-didehydrobenzene and to understand the influence of perturbations (substituents,[2,7,9b] heteroatoms,[8,9] annelation[9]) on these systems. Less is known about *meta*-benzyne **1** and its derivatives. Early trapping experiments are inconclusive concerning the question whether **1** exists as a monocyclic biradical **1a** or as a highly strained bicyclic anti-Bredt olefin **1b**.[10]

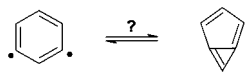

Direct investigations of *meta*-benzyne have become possible only recently. Negative ion photoelectron spectra (NIPES) show an extended progression with irregular peak spacing at ca. 300 cm^{-1}, which could not be reproduced using standard harmonic or Morse potentials.[4a] As a possible interpretation, it has been suggested that this vibrational structure is mainly due to a stretching mode involving the dehydrocarbons. This implies a structure with intermediate C1C3 bond length. However, NIPES results for *meta*-benzyne are considerably more complex and confusing than for the *ortho*- and *para*-isomers, which have also been measured by Wenthold, Squires, and Lineberger.[4a] The IR spectrum of **1** has been measured in an argon matrix at 10 K by Sander et al. starting from two independent precursors.[1a,2f] The IR spectrum calculated at the CCSD(T)/6-31G* level by Cremer et al. nicely reproduces the measured data, which therefore have been interpreted in favor of structure **1a** (R_{C1C3} = 210.6 pm).[1a,2f,6c] Nonetheless, the existence of a bicyclic isomer **1b** still remains a matter of debate.[11]

Computational studies continue to play an important role for investigations of didehydrobenzenes and their derivatives.[6−9] It has been known for a long time that calculated equilibrium geometries of *meta*-benzynes strongly depend on the level of theory applied, especially with regard to the distance of the radical centers. From a chemical point of view, this is the most important geometrical feature as it allows to rationalize the influence of perturbations (e.g., substituents) on the properties and reactivity of *meta*-didehydrobenzene.[7−9] In most studies, it seems to be common practice to optimize geometries at the density functional theory (DFT) and at the multiconfigurational self-consistent field (MCSCF) level of theory and to 'judge' the quality of the structures by higher level single-point calculations (MR−CI, CASPT2, CCSD(T), etc.). The lower energy structure is generally assumed to be of higher accuracy and taken for a more chemically oriented analysis. In addition, it is found in many cases that DFT performs better in this regard than MCSCF or more demanding CCSD(T) calculations, although there is no general agreement about which functional should be preferred.[12] It must be pointed out, however, that this approach bears some risks and may lead to unphysical interpretations in the case of *meta*-benzynes. Because the potential-energy surface in the region between **1a** and **1b** is very flat, systematic deviations in 'secondary' geometrical parameters (e.g., CH bond lengths), which are usually of little relevance, may give stronger contributions to the total energy than

* To whom correspondence should be addressed. E-mail: Wolfram.Sander@ruhr-uni-bochum.de.

10.1021/jp012100c CCC: $20.00
Published on Web 10/20/2001

variations in the structural features of interest (in this case, the C1C3 internuclear separation). Therefore, although the total energy at high levels of theory may be lower for the DFT structure, it is not clear a priori that this structure can reasonably be taken as a basis for a more detailed analysis.

In this work, we describe the results of our calculations on *meta*-benzyne focusing on the C1C3 internuclear distance. Constrained geometry optimizations are carried out employing four commonly used DFT functionals (B3LYP, BLYP, B3PW91, BPW91) in combination with small- (cc-pVDZ) and medium-sized (cc-pVTZ) basis sets over a wide range of C1C3 separations (130−240 pm). The potential-energy curves are compared to that calculated at the CASSCF level of theory. MR−CI, CASPT2, and CCSD(T) single-point energies are calculated for several DFT and CASSCF structures along the cyclization coordinate. This procedure allows us to determine a small interval for the most probable C1C3 distance. NBO population analysis[13] and topological analysis of the electron density distribution[14] for a reliable structure of **1** are carried out to learn more about the mechanism of spin coupling that leads to a singlet ground state of *meta*-benzyne.[6]

2. Computational Procedures

Constrained geometry optimizations are done by freezing the distance of the radical centers and optimizing all remaining degrees of freedom within the C_{2v} point group symmetry of the molecule. The effect of removing all symmetry constraints has been tested frequently, but in no case led to a different structure. Geometries of stationary points are fully optimized using analytic derivatives in most cases. Tight convergence criteria for gradients and a full (99, 590) integration grid, having 99 radial shells per atom and 590 angular points per shell, are used throughout to obtain accurate values for geometries and low-frequency vibrational modes. Solutions of spin-restricted DFT and HF calculations are tested for internal and external instabilities with the help of the Hermitian stability matrixes **A** and **B**.[15] All RHF and RDFT results turn out to be internally stable, but for larger C1C3 separations **B** possesses one (sometimes even two) negative eigenvalues λ, indicating a breaking of the constraint $\psi_\alpha = \psi_\beta$. In those cases, geometries are reoptimized at the spin-unrestricted (U) level, which leads to an energy lowering ΔE_{UR} (see Tables 1S−9S). Both parameters, λ and ΔE_{UR}, served as indicators for the degree of instability of the spin-restricted (R) solution in previous work.[12a]

Explorative calculations are made using Dunning's cc-pVDZ basis set, and the results are compared to that obtained with the larger cc-pVTZ basis set; contractions read (9s4p1d/4s1p)-[3s2p1d/2s1p] and (10s5p2d1f/5s2p1d)[4s3p2d1f/3s2p1d].[16] Two gradient-corrected (GGA) functionals, BPW91[17,18] and BLYP,[17,19] are employed in this work, both of which use the Becke exchange functional[17] (gradient-corrected Slater exchange to account for nonlocal exchange effects)[20] in combination with the Perdew−Wang (1991) gradient-corrected correlation functional[18] and the Lee−Yang−Parr correlation functional,[19] respectively. In addition, two hybrid functionals (B3LYP and B3PW91) are tested.[21] All functionals are used as implemented in Gaussian 98[22] without any change of parameters.

DFT calculated energy profiles for the cyclization **1a** ↔ **1b** are compared to that obtained at the CASSCF level of theory.[23] The active space contains the bonding and antibonding combination of the radical lobes in the case of CASSCF(2,2) and in addition the six π orbitals for CASSCF(8,8). RHF and RMP2 calculations are included for comparison, because in previous work similar structures for *meta*-benzyne at the RMP2 and CCSD(T) level have been reported.[6c]

To get an impression of the quality of the energy profiles calculated with different methods, RCCSD(T)/cc-pVTZ[24,28] and BCCD(T)/cc-pVTZ[24,25,28] single-point energies are determined for a number of structures along the cyclization coordinate. Brueckner orbitals[26] eliminate contributions from single excitations in the coupled-cluster ansatz, and the energy difference obtained with the wave function expanded in Hartree−Fock or Brueckner orbitals is usually taken as an indicator for nondynamic electron correlation, not covered by the single-reference coupled-cluster approach.[25,27,28] For all C1C3 separations, we find that the differences between the absolute energies computed at the BCCD(T) and CCSD(T) level are below 0.42 kcal/mol with the CCSD(T) energy being lower in all cases. In addition, all T_1 diagnostics are ≤ 0.02 (see Tables 13S and 14S).[29,28]

For larger C1C3 separations, multireference configuration−interaction (MR−CI) is expected to be the most reliable computational method.[30] In the following, MR−CI is used as a shorthand notation for CAS(8,8)-CISD+Q/cc-pVTZ, the internally contracted MR−CI of Werner et al. including all single and double excitations from a CASSCF(8,8) reference space.[31] Furthermore, the effect of quadruple excitations is estimated by the Davidson correction scheme.[32]

Although multireference perturbation theory (CASPT2)[33] is not expected to give reliable results for dissociation reactions,[30,33] CASPT2/cc-pVTZ calculations have been carried out because this method is frequently used for calculations on didehydrobenzenes and their derivatives. The original RS2 method of Werner (only the doubly external configurations are internally contracted)[33c] was used for these calculations using a CASSCF-(8,8) reference as outlined above.

Geometry optimizations and single-point energy calculations have been carried out with the Gaussian 98[22] and Molpro 2000.1[34] electronic structure program suites, respectively. Electron densities for AIM analysis have been recalculated using Cartesian d and f functions (7D, 10F), whereas pure functions are used in all other cases. The AIM 2000 program of Biegler-König et al. was used for topological analysis of the electron density distribution.[35]

3. Energy Profiles for the Cyclization of *meta*-Benzyne

Energy profiles obtained at the DFT level are shown in Figures 1 and 2, (low level) ab initio results are given in Figure 3. These may be compared to the benchmark calculations depicted in Figure 4.

The topology of the potential-energy curves and the equilibrium C1C3 distance strongly depend on the level of theory applied. Equilibrium structures are summarized in Table 1. Several aspects of these potential-energy curves will be discussed in turn.

Comparison of Methods. HF−SCF gives a qualitatively wrong description of the potential-energy surface (PES) and strongly overemphasizes bonding between the radical centers. Even the simplest two-configurational approach gives rise to a very different structure with the C1C3 separation being 70 pm larger. However, the slope of the CASSCF(2,2) PES along the cyclization coordinate is too steep. Enlargement of the active space to CASSCF(8,8) does not result in any improvements, and inclusion of dynamic electron correlation (which makes the potential-energy curves flatter, see Figure 2S) is indispensable for a proper description of the *meta*-benzyne cyclization.[8a,b]

Although RMP2/cc-pVTZ leads to a reasonable equilibrium geometry ($R_{C1C3} = 208.3$ pm), the descent of the PES is still too steep. Because MP2 results based on an externally unstable RHF wave function (vide infra) are questionable[36] and test

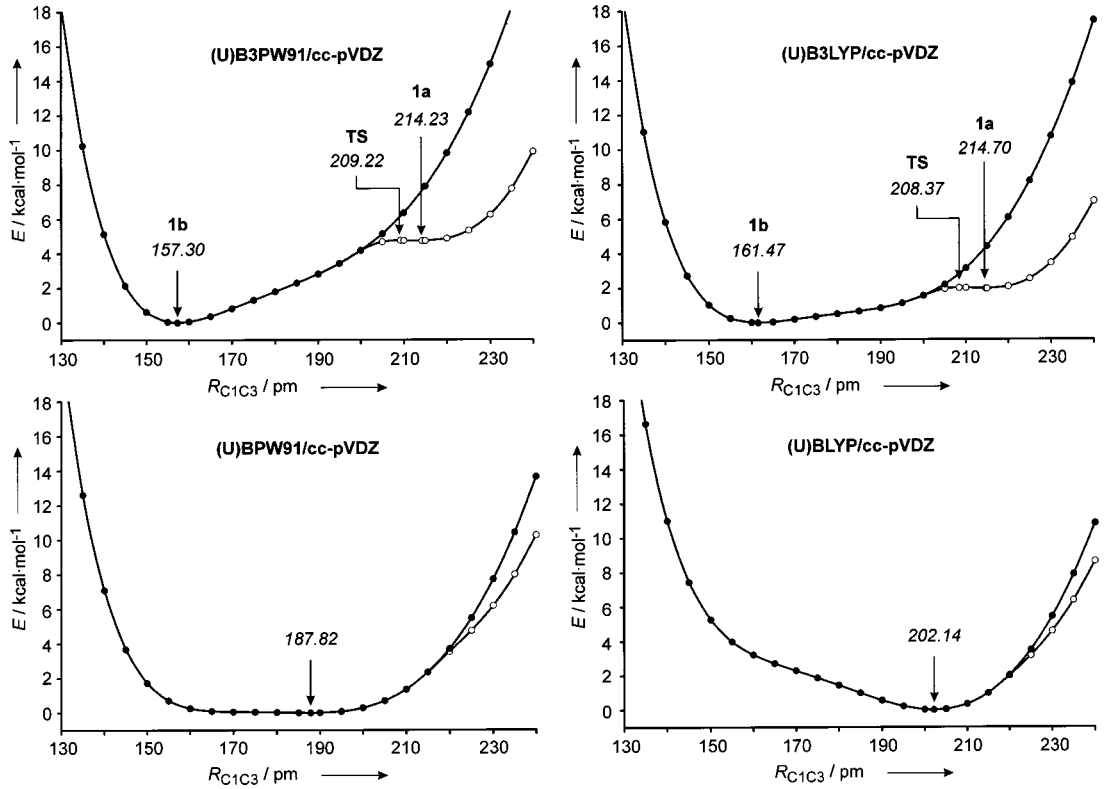

Figure 1. Energy profiles for the cyclization of *meta*-benzyne calculated at the DFT/cc-pVDZ level of theory. For absolute energies see Tables 1S−4S.

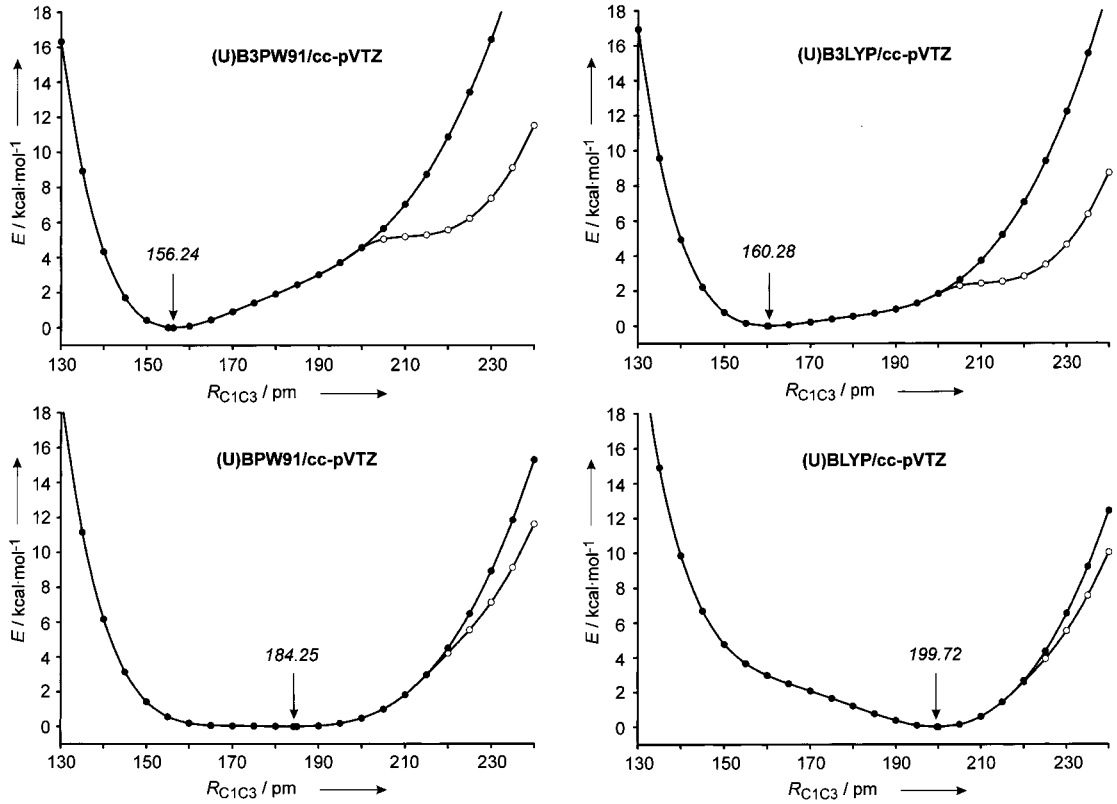

Figure 2. Energy profiles for the cyclization of *meta*-benzyne calculated at the DFT/cc-pVTZ level of theory. For absolute energies see Tables 5S−8S.

calculations at the UMP2 level reveal substantial spin contamination, this method is not considered any further here. It suffices to mention that the RMP2 calculated IR spectrum of *meta*-benzyne does not even agree qualitatively with the vibrational spectrum measured by Sander et al. (see Supporting Information).[2f]

All DFT methods come closer to the benchmark calculations than HF−SCF, but depending on the functional, very different

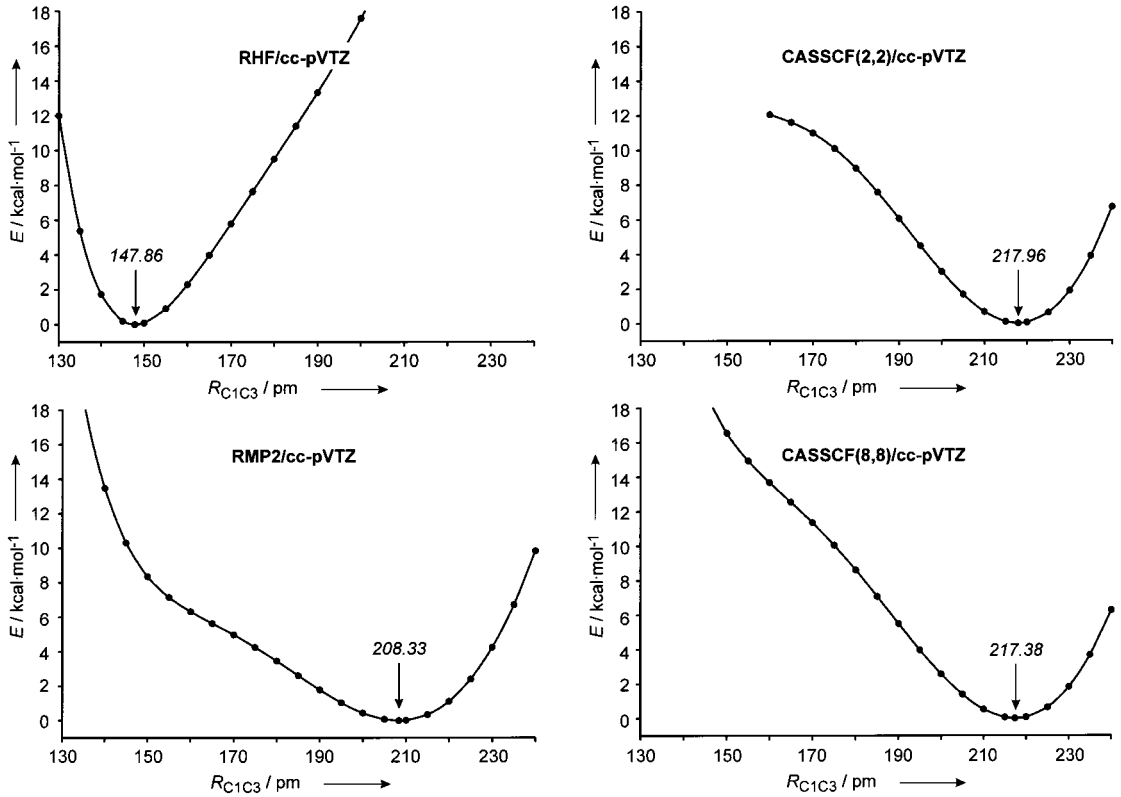

Figure 3. Energy profiles for the cyclization of *meta*-benzyne calculated at several levels of wave function theory. For absolute energies see Tables 9S−12S.

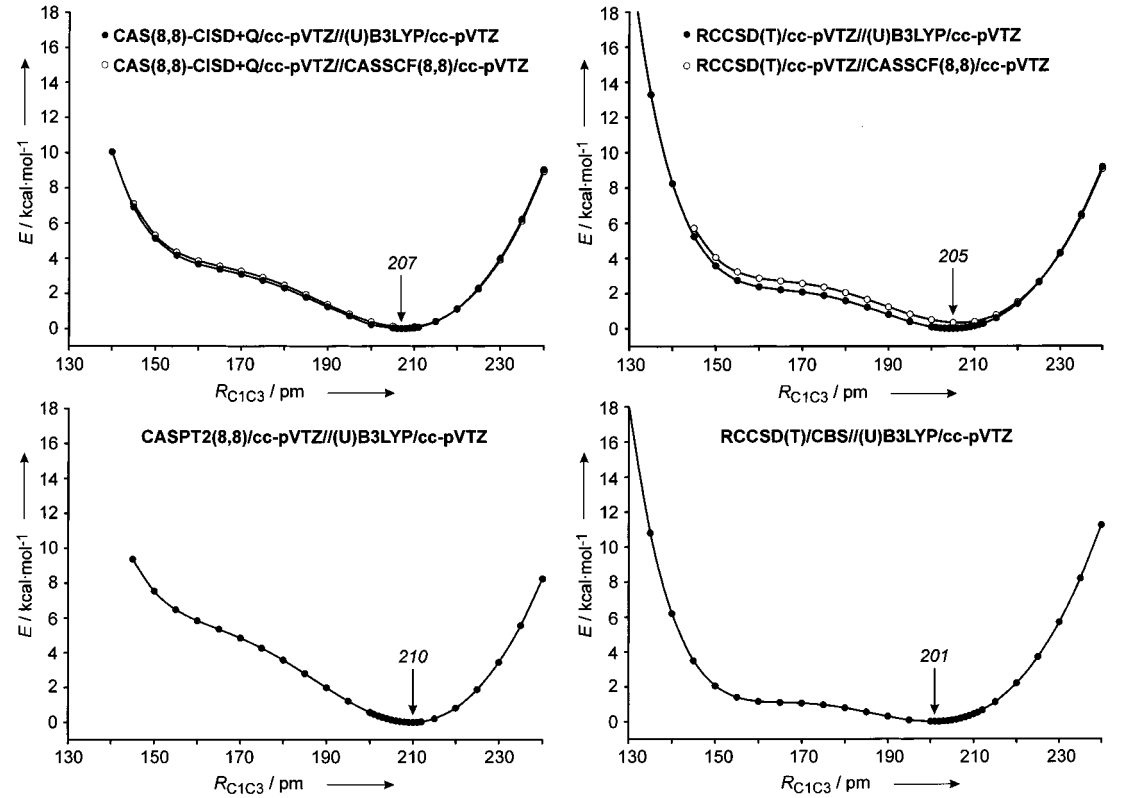

Figure 4. Energy profiles for the cyclization of *meta*-benzyne calculated at highly correlated levels of theory for a number of (U)B3LYP/cc-pVTZ and CASSCF(8,8)/cc-pVTZ optimized structures.

results are obtained. The question whether pure or hybrid functionals show a better performance for calculations on biradicals is still discussed controversially.[12] For *meta*-benzyne, we find that pure GGA protocols are superior to hybrid DFT methods. The energy profile obtained at the BLYP level is very similar to that obtained with the much more expensive CCSD(T) or MR−CI methods, and BLYP appears to be the functional of choice for aromatic *meta*-biradicals. It is also found that the vibrational spectrum calculated at the BLYP/cc-pVTZ level fits excellently the measured IR spectrum, whereas agreement

TABLE 1: Equilibrium Structures (Distances *R* in pm and Angles *A* in Degrees) of *meta*-Benzyne Calculated at Different DFT and Ab Initio Levels of Theory

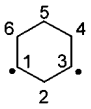

method	basis	R_{C1C3}	R_{C1C2}	R_{C3C4}	R_{C4C5}	R_{C2H7}	R_{C4H8}	R_{C5H9}	A_{C1C2C3}	A_{C2C3C4}	A_{C3C4C5}	A_{C4C5C6}
HF	aug-cc-pVTZ	147.8	133.5	138.2	140.2	107.1	106.8	107.6	67.3	164.4	105.7	112.5
HF	cc-pVTZ	147.9	133.5	138.1	140.2	107.1	106.8	107.6	67.3	164.4	105.7	112.6
HF	aug-cc-pVDZ	148.9	134.4	138.9	140.8	107.8	107.6	108.3	67.3	164.3	105.8	112.6
HF	cc-pVDZ	148.8	134.5	138.7	140.8	108.1	107.7	108.5	67.2	164.4	105.7	112.6
MPW1PW91	cc-pVTZ	154.9	134.3	137.5	140.5	108.2	107.8	108.5	70.4	161.2	107.7	111.7
MPW1PW91	cc-pVDZ	155.9	135.3	138.3	141.2	109.2	108.8	109.4	70.3	161.2	107.7	111.8
B3PW91	aug-cc-pVTZ	156.4	134.4	137.6	140.7	108.3	108.0	108.6	71.1	160.5	108.1	111.6
B3PW91	cc-pVTZ	156.2	134.5	137.6	140.7	108.4	108.0	108.6	71.0	160.7	108.0	111.7
B3PW91	aug-cc-pVDZ	157.9	135.4	138.4	141.3	109.1	108.8	109.4	71.3	160.3	108.2	111.7
B3PW91	cc-pVDZ	157.3	135.5	138.4	141.4	109.4	108.9	109.6	71.0	160.7	108.0	111.8
B3P86	cc-pVTZ	156.3	134.3	137.5	140.5	108.2	107.9	108.5	71.1	160.5	108.1	111.6
B3P86	cc-pVDZ	157.4	135.4	138.3	141.2	109.3	108.9	109.5	71.1	160.5	108.1	111.7
SVWN	cc-pVTZ	156.9	134.4	137.0	140.2	109.3	108.9	109.5	71.4	160.2	108.4	111.5
SVWN	cc-pVDZ	158.1	135.6	137.9	141.0	110.4	109.9	110.5	71.4	160.1	108.4	111.6
MPW1LYP	cc-pVTZ	159.0	134.3	137.6	140.6	108.1	107.7	108.3	72.6	159.2	108.7	111.6
MPW1LYP	cc-pVDZ	160.1	135.3	138.4	141.4	109.3	108.8	109.4	72.5	159.2	108.7	111.7
B3LYP	cc-pVTZ	160.3	134.4	137.6	140.7	108.2	107.9	108.5	73.2	158.7	109.0	111.5
B3LYP	aug-cc-pVDZ	163.4	135.4	138.5	141.4	109.1	108.8	109.4	74.2	157.6	109.5	111.6
B3LYP	cc-pVDZ	161.5	135.4	138.5	141.5	109.4	109.0	109.6	73.2	158.7	109.0	111.6
BPW91	cc-pVTZ	184.3	135.5	137.4	140.7	108.8	108.8	109.3	85.7	147.4	113.9	111.8
BPW91	cc-pVDZ	187.8	136.5	138.2	141.4	109.8	109.8	110.3	86.9	146.2	114.3	112.0
BP86	cc-pVTZ	190.4	136.0	137.4	140.8	108.9	109.0	109.5	88.9	144.6	114.9	112.1
BP86	cc-pVDZ	193.3	137.0	138.3	141.5	109.9	110.0	110.5	89.7	143.8	115.2	112.3
BLYP	cc-pVQZ	199.5	136.6	137.4	140.9	108.4	108.7	109.2	93.8	140.5	116.1	112.9
BLYP	aug-cc-pVTZ	199.5	136.7	137.4	140.9	108.5	108.8	109.2	93.8	140.5	116.1	112.9
BLYP	cc-pVTZ	199.7	136.7	137.4	140.9	108.5	108.8	109.2	93.9	140.4	116.2	112.9
BLYP	aug-cc-pVDZ	202.8	137.8	138.4	141.7	109.4	109.7	110.2	94.8	139.6	116.4	113.1
BLYP	cc-pVDZ	202.1	137.7	138.4	141.7	109.7	109.9	110.4	94.4	139.9	116.4	113.1
MP2	cc-pVTZ	208.3	136.6	136.8	139.6	107.2	107.6	108.9	99.4	135.7	117.8	113.7
MP2	aug-cc-pVDZ	214.6	138.8	138.8	141.5	108.9	109.3	109.7	101.2	134.1	118.1	114.2
MP2	cc-pVDZ	214.3	138.6	138.7	141.2	109.1	109.4	109.9	101.3	134.1	118.1	114.3
UB3PW91	cc-pVDZ	214.2	137.7	137.6	140.3	108.9	109.3	109.6	102.1	133.7	117.4	115.6
UB3LYP	cc-pVDZ	214.7	137.9	137.7	140.5	108.9	109.3	109.6	102.2	133.7	117.4	115.5
CASSCF(8,8)	cc-pVTZ	217.4	137.4	137.8	139.5	106.7	107.2	107.5	104.5	131.7	118.0	116.0
CASSCF(8,8)	cc-pVDZ	219.7	138.2	138.5	140.1	107.6	108.1	108.4	105.2	131.1	118.1	116.2
CASSCF(2,2)	cc-pVTZ	218.0	136.7	136.8	138.6	106.7	107.2	107.5	105.7	131.0	117.7	116.9
CASSCF(2,2)	cc-pVDZ	220.0	137.5	137.6	139.2	107.7	108.1	108.4	106.3	130.5	117.8	117.1

becomes worse with methods that predict a stronger bond between the radical centers (Figure 5). A similar finding has been reported for several substituted derivatives of **1**.[2c]

It is well known that basis set convergence is less of an issue in DFT than in wave function theory.[37d] Therefore, the changes observed in the energy profiles upon enlargement of the basis sets from cc-pVDZ to cc-pVTZ are rather insignificant for all DFT methods. However, at the UB3LYP/cc-pVDZ and UB3PW91/cc-pVDZ level, a flat, double-well potential is found with a second minimum energy structure at C1C3 separations around 215 pm in both cases. The barrier between the two minima is only 0.04 and 0.03 kcal/mol, respectively, and disappears completely when larger basis sets are employed.

Wave Function Stability. For both HF−SCF and all DFT methods, the R solution at the equilibrium geometry turns out to be stable. Table 2 gives all six eigenvalues of the stability matrixes **A** and **B** for the minimum energy structures.

Because of the different distances of the radical centers, these values cannot be compared directly, and one has to look at solutions for a fixed distance R_{C1C3} to compare differences in the stability among the different methods (Table 3). All DFT methods are more stable toward spin-symmetry breaking than the SCF wave function, which becomes unstable for C1C3 separations above 170 pm.

The R solutions for the hybrid methods are stable for $R_{C1C3} \leq 200$ pm, and instabilities for the pure DFT methods arise for distances above 215 pm. The same trend can be observed for the energy differences ΔE_{UR}, which are large at the Hartree−Fock level, moderate for the hybrid methods, and small for the GGA functionals. A quadratic relationship between ΔE_{UR} and λ has been proposed by Cremer et al. and therefore λ_{min} shows the same tendency.[12a] These findings are in line with earlier investigations by Bauernschmitt and Ahlrichs[15b] and Cremer et al.[12a] The degree of instability of the RDFT solution directly reflects shortcomings of the respective approximate exchange−correlation functional. For the exact functional, no UR-bifurcation (and associated artifacts like nonvanishing spin magnetization densities for the $S = 0$ case) should occur, and the RDFT solution should give an exact description even in pathological cases.[12a,15] However, no clear correlation between performance and stability seems to exist, and usually, results obtained with the local spin density approximation (e.g., SVWN) are more stable than GGA functionals, which is probably due to a systematic overestimation of electron correlation in the former case.[12a,15] Generally, the LYP correlation functional gives

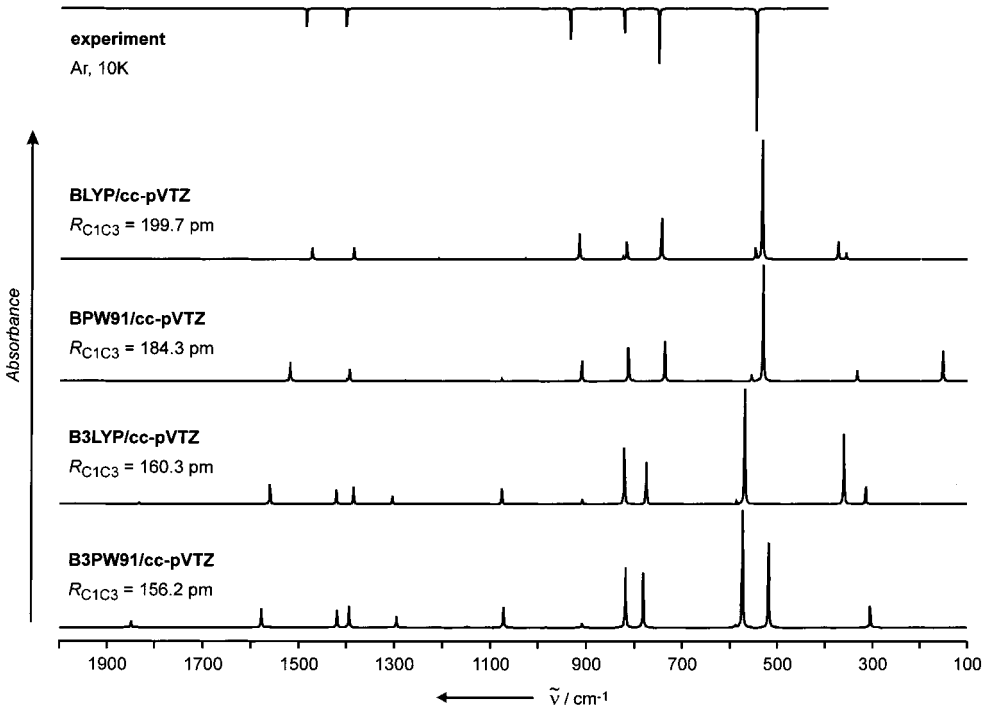

Figure 5. Vibrational spectra of *meta*-benzyne calculated at different DFT levels. The published IR spectrum[2f] (Ar, 10K) is shown schematically for comparison.

TABLE 2: Absolute Energies (in Hartrees) for the Equlibrium Geometries of 1 Calculated at Different DFT Levels of Theory. Eigenvalues of the Hermitian Stability Matrixes A and B Are Given as λ_1 to λ_6

method	basis	R_{C1C3}	E_{el}	λ_1	λ_2	λ_3	λ_4	λ_5	λ_6
HF	cc-pVTZ	147.9	−229.451926	0.0220[b]	0.0978[c]	0.1418[b]	0.1620	0.1623	0.1639
HF	aug-cc-pVDZ	148.9	−229.400993	0.0193[b]	0.0960[c]	0.1391[b]	0.1589	0.2021	0.2159
HF	cc-pVDZ	148.8	−229.394196	—[a]	—[a]	—[a]	—[a]	—[a]	—[a]
MPW1PW91	cc-pVTZ	154.9	−230.913217	0.0978[b]	0.1144[c]	0.1398[d]	0.1658	0.1663	0.2416
MPW1PW91	cc-pVDZ	155.9	−230.854779	0.0954[b]	0.1141[c]	0.1404[d]	0.1657	0.1668	0.2431
B3PW91	cc-pVTZ	156.2	−230.881734	0.1040[b]	0.1159[c]	0.1384[d]	0.1628	0.1660	0.2373
B3PW91	aug-cc-pVDZ	157.9	−230.830384	0.1016[b]	0.1144[c]	0.1366[d]	0.1551	0.1601	0.1630
B3PW91	cc-pVDZ	157.3	−230.822260	0.1016[b]	0.1154[c]	0.1389[d]	0.1632	0.1659	0.2385
B3P86	cc-pVTZ	156.3	−231.688398	0.1065[b]	0.1169[c]	0.1390[d]	0.1628	0.1665	0.2370
B3P86	cc-pVDZ	157.4	−231.627925	0.1040[b]	0.1163[c]	0.1393[d]	0.1632	0.1664	0.2382
SVWN	cc-pVTZ	156.9	−229.638224	0.1250[c]	0.1368[d]	0.1491[b]	0.1514	0.1679	0.2306
SVWN	cc-pVDZ	158.1	−229.558453	0.1236[c]	0.1368[d]	0.1461[b]	0.1518	0.1678	0.2321
MPW1LYP	cc-pVTZ	159.0	−230.841500	0.1024[b]	0.1186[c]	0.1381[d]	0.1616	0.1668	0.2297
MPW1LYP	cc-pVDZ	160.1	−230.774266	0.0989[b]	0.1177[c]	0.1381[d]	0.1619	0.1666	0.2308
B3LYP	cc-pVTZ	160.3	−230.973401	0.1083[b]	0.1201[c]	0.1366[d]	0.1586	0.1675	0.2265
B3LYP	aug-cc-pVDZ	163.4	−230.917147	0.1052[b]	0.1190[c]	0.1331[d]	0.1542	0.1648	0.2066
B3LYP	cc-pVDZ	161.5	−230.906554	0.1050[b]	0.1192[c]	0.1366[d]	0.1588	0.1674	0.2275
BPW91	cc-pVTZ	184.3	−230.949820	—[a]	—[a]	—[a]	—[a]	—[a]	—[a]
BPW91	cc-pVDZ	187.8	−230.888863	0.0627[c]	0.1154[b]	0.1201[d]	0.1414	0.1789	0.1797
BP86	cc-pVTZ	190.4	−230.973635	0.0547[c]	0.1182[d]	0.1189[b]	0.1403	0.1704	0.1788
BP86	cc-pVDZ	193.3	−230.911624	0.0500[c]	0.1171[b]	0.1181[d]	0.1411	0.1672	0.1795
BLYP	cc-pVTZ	199.7	−230.885963	0.0318[c]	0.1118[d]	0.1200[b]	0.1402	0.1496	0.1660
BLYP	aug-cc-pVDZ	202.8	−230.828467	0.0279[c]	0.1080[d]	0.1172[b]	0.1172	0.1440	0.1573
BLYP	cc-pVDZ	202.1	−230.814642	0.0286[c]	0.1105[d]	0.1173[b]	0.1402	0.1486	0.1630

[a] The stability test could not be carried out because of two degenerate eigenvalues λ. [b] $^1A_1 \rightarrow {}^3A_1$. [c] $^1A_1 \rightarrow {}^3B_2$. [d] $^1A_1 \rightarrow {}^3B_1$.

solutions which are slightly more stable than that obtained with PW91.[12a] In contrast to earlier investigations, we find that an extension of the basis set decreases the stability of the RDFT solution as is reflected by both parameters λ_{min} and ΔE_{UR}.[12a] However, the effects are small, and the differences between the ΔE_{UR} values are only some tenths of a kcal. Also given in Table 3 are $\langle S^2 \rangle$ expectation values determined from the Kohn−Sham orbitals. Because it has been shown that these quantities are only of limited diagnostic value to assess spin contamination, we simply note that they follow the same tendency as ΔE_{UR} and λ without giving any physical significance to their exact size.[12a]

CCSD(T), CASPT2, and MR−CI. The potential-energy curves determined at all three levels of theory show a similar topology, and they agree that the equilibrium distance between the radical centers is around 205 ± 5 pm. Some interesting points may be noted, however.

As shown in Figure 1S, there is a strongly alternating behavior for the calculated minimum energy structures in the series HF, MP2, CCSD, and CCSD(T); the lowest energies are obtained for C1C3 distances of 150 ± 4, 210 ± 1, 155 ± 4, and 205 ± 1 pm, respectively (if not mentioned otherwise, all values are given for (U)B3LYP/cc-pVTZ geometries). It is well known that (noniterative) inclusion of triple excitations increases the

TABLE 3: Stabilities of Different DFT Solutions Compared to that of the HF−SCF Wavefunction[a]

		$R_{C1C3} = 195$ pm			$R_{C1C3} = 210$ pm			$R_{C1C3} = 240$ pm		
method	R_{min}	λ_{min}	ΔE_{UR}	$\langle S^2 \rangle$	λ_{min}	ΔE_{UR}	$\langle S^2 \rangle$	λ_{min}	ΔE_{UR}	$\langle S^2 \rangle$
RHF/cc-pVTZ	170	−0.1189	19.7	0.7652	−0.1700	37.5	0.9009	−0.2267	63.5	0.9917
B3PW91/cc-pVDZ	195	−[b]			−[b]	1.61	0.3854	−0.0659	12.2	0.8184
B3PW91/cc-pVTZ	195	0.0116			−[b]	1.84	0.4102	−0.0665	12.5	0.8261
B3LYP/cc-pVDZ	200	0.0166			−[b]	1.13	0.3229	−0.0627	10.4	0.7835
B3LYP/cc-pVTZ	200	0.0146			−0.0218	1.30	0.3451	−0.0629	10.7	0.7922
BPW91/cc-pVDZ	215	0.0425			0.0098			−0.0274	3.38	0.6161
BPW91/cc-pVTZ	210	0.0397			0.0076			−0.0287	3.69	0.6366
BLYP/cc-pVDZ	215	0.0456			0.0130			−0.0239	2.21	0.5081
BLYP/cc-pVTZ	215	0.0431			0.0111			−0.0247	2.38	0.5277

[a] R_{min} gives the smallest dehydrocarbon distance in pm that is found to be externally stable, λ_{min} is the smallest eigenvalue of the B-matrix. $\langle S^2 \rangle$ values for the UDFT solutions and energy differences ΔE_{UR} in kcal/mol are given for comparison. [b] The stability test could not be carried out because of two degenerate eigenvalues λ.

radius of convergence of the coupled-cluster method significantly.[28] On the other hand, it is not clear whether inclusion of higher order excitations may again favor smaller separations, and therefore the CCSD(T) results are not conclusive a priori.

The situation is less troublesome for the MR−CI approach (Table 15S, 16S, and Figure 2S). The lowest energies in the series CASSCF(8,8), CAS(8,8)-CISD, and CAS(8,8)-CISD+Q are found for C1C3 separations of 215 ± 4, 210 ± 1, and 207 ± 1 pm. As mentioned above, the PES becomes successively flatter with inclusion of higher order excitations. The cluster correction leads to a significant energy lowering (ca. 85 kcal/mol on average), and therefore even the quite large CAS(8,8)-CISD, which contains nearly 18,000,000 contracted configurations, does not cover all important terms.

CASPT2 is known to suffer from systematic errors proportional to the number of unpaired electrons, and CASPT2 artificially favors separation of electrons.[33a,33b] Accordingly, the energy increases more strongly with decreasing R_{C1C3} than at the CCSD(T) and MR−CI level, and the lowest energy structure is found for a C1C3 separation of 210 pm.

Despite the shortcomings of each individual method, the close similarity of the energy curves shown in Figure 4 confirms that the basic conclusions are not affected significantly by the different ways of the *N*-electron treatment. It remains to be checked whether the cc-pVTZ basis set is sufficiently flexible to give definitive results.[37] Because of the slow convergence of the electron−electron interaction (cusp), which asymptotically converges as $(l + {}^1/_2)^{-4}$ (see refs 38, 37g, and 37h) with l the maximum angular momentum function in the one-electron space, and taking into account the strong influence of dynamic electron correlation on the shape of the potential-energy curve (vide supra), very large basis sets may be necessary to obtain definitive answers. Since the CCSD(T) method scales as N^6 for solution of the CCSD equations and requires an additional N^7 step for the perturbative calculation of the triple excitations (with N the number of basis functions),[28] reliable basis sets (e.g., *spdfgh*) cannot be employed in the present context (the cc-pV5Z basis set for *meta*-benzyne already consists of 766 functions). Several extrapolation schemes to the complete basis set (CBS) limit have been proposed in the literature.[37] Because cc-pVDZ recovers only a very small fraction of the correlation energy and because cc-pVTZ is generally considered the 'minimal basis set' for correlated calculations,[37] most extrapolations require at least cc-pVQZ data. Nevertheless, Truhlar et al. developed a simple extrapolation scheme starting from CCSD(T)/cc-pVDZ and CCSD(T)/cc-pVTZ calculations.[37e,37f] For the atomization energies of 29 different (open- and closed-shell) molecules, he obtained values close to cc-pV5Z results with a mean unsigned error of 1.76 kcal/mol relative to the complete basis set limit.[37e] The extrapolated energies according to this scheme (see refs 37e, 37f, and Table 18S for details) are denoted as CCSD(T)/CBS, and the potential-energy curve is shown in Figure 4. Since there is no way to decide whether the Truhlar extrapolation leads to over- or undercorrection for the *meta*-benzyne molecule, the results should be taken with some caution. However, they may suffice to get a qualitative impression of the effects of basis set enlargement. It is evident that the CBS potential-energy curve is even flatter than that obtained with the cc-pVTZ basis set. The minimum energy structure is found for $R_{C1C3} = 211 \pm 1$ pm at the CCSD(T)/cc-pVDZ level, and this distance is reduced to 205 ± 1 pm using the cc-pVTZ basis set and further to 201 ± 1 pm in the CBS limit. Despite these differences, the qualitative conclusions are not altered and all calculations agree that a bicyclic isomer **1b** does not exist and *meta*-benzyne is characterized by a flat single-well potential-energy curve with a minimum energy structure for $R_{C1C3} = 205 \pm 5$ pm.

4. The Electronic Structure of *meta*-Benzyne

The question for which distance between the radical centers a bond should be drawn is somewhat philosophical in nature and cannot be answered by quantum chemical calculations alone. The theory of atoms in molecules[14] gives a definition of a chemical bond and of molecular structure in terms of the topology of the molecular charge distribution $\rho(\mathbf{r})$: The presence of a (3,−1) bond critical point (BCP) between two (3,−3) nuclear attractors of the gradient vector field $\nabla\rho(\mathbf{r})$, which implies the connection of these attractors by a maximum electron density path (MED), is usually taken as a necessary condition for the existence of a covalent bond. To distinguish between covalent and closed-shell interactions, a negative energy density $H(\mathbf{r}) = G(\mathbf{r}) + V(\mathbf{r})$ at the BCP is required as well (sufficient condition).[14d,14e] If this is fulfilled, the MED is called a bond path. The set of nuclear attractors and the MEDs connecting them define a molecular graph. Two different geometries (configurations) belong to the same molecular structure if their molecular graphs are topologically equivalent, that is, structure is defined as an equivalence class of molecular graphs. Each structure is associated with a structural region in nuclear configuration space. The structural regions form a dense, open subset of this space, and each configuration that belongs to a structural region is called a regular point. Changes in molecular structure are abrupt and discontinuous processes via topologically unstable catastrophe points (which belong to the complementary of the set of regular points).[14] Figure 6 shows the gradient vector field of **1** calculated with the B3LYP/cc-pVTZ density for C1C3 distances of 150 and 160 pm.

For 150 pm, two (3,+1) ring critical points (RCP) are found and C1 and C3 are connected by a bond path. For a distance of

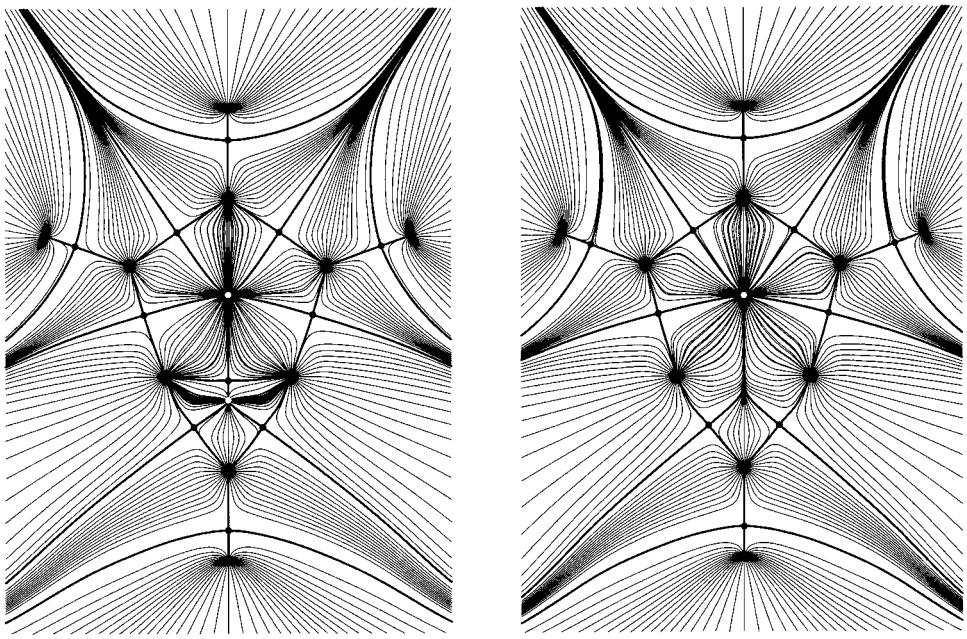

Figure 6. Display of the gradient vector field $\nabla\rho(\mathbf{r})$ of the charge density distribution of **1** in the molecular plane for C1C3 distances of 150 and 160 pm. For the smaller distance, a bond path (bold line) and a BCP (black circle) is found between C1 and C3. In addition, two RCPs (white circles) exist. For the larger distance, only one RCP is found and no MED path connects the radical centers.

TABLE 4: NBO Analysis of *meta*-Benzyne for Two Different Dehydrocarbon Separations at the B3LYP/cc-pVTZ Level of Theory[a]

		$R_{C1C3} = 160$ pm					$R_{C1C3} = 210$ pm				
φ_i	φ_j	occ. φ_i	occ. φ_j	F_{ij}	$\Delta\epsilon_{ij}$	$E^{(2)}$	occ. φ_i	occ. φ_j	F_{ij}	$\Delta\epsilon_{ij}$	$E^{(2)}$
	σ^*_{C2H7}		0.0614	0.156	0.72	40.28		0.0508	0.115	0.59	26.00
	σ^*_{C1C2}		0.0303	0.110	0.88	16.09		0.0404	0.122	0.73	23.56
σ_{C1C3}	σ^*_{C4H8}	1.8353	0.0224	0.081	0.78	9.77	1.8061	0.0205	0.069	0.60	9.13
	σ^*_{C4C5}		0.0165	0.050	0.86	3.35		0.0216	0.071	0.71	8.27
	σ^*_{C5H9}		0.0179	0.032	0.78	1.52		0.0192	0.020	0.61	0.78
	σ^*_{C3C4}		0.0165	0.025	0.90	0.81		0.0151	0.033	0.76	1.65
σ_{C1C2}		1.9568		0.089	0.89	10.86	1.9497		0.084	0.66	12.73
σ_{C3C4}	σ^*_{C1C3}	1.9879	0.0818	0.041	0.90	2.29	1.9855	0.1540	0.041	0.67	2.92
σ_{C4H8}		1.9795		0.032	0.71	1.76	1.9648		0.023	0.45	1.46
σ_{C4C5}		1.9797		0.035	0.87	1.74	1.9708		0.041	0.62	3.10

[a] Fock matrixelements F_{ij} and orbital energy differences $\Delta\epsilon_{ij}$ between several NBOs φ_i (donor) and φ_j (acceptor) are given in atomic units, second-order interaction energies $E^{(2)}$ are given in kcal/mol.

160 pm, only one RCP is found and no MED path connects the radical centers. Therefore, the structural change (bifurcation) occurs around $R_{C1C3} = 155$ pm and, according to the AIM scheme, all structures with larger distances between C1 and C3 are best represented by a monocyclic formula **1a**.

Biradical Character. For a simple two configurational wave function, the biradical character χ may easily be defined in terms of natural orbital occupation numbers (*NOON*s)[39] as $\chi = \{NOON(a)/NOON(b)\} \times 100$ with $NOON(a) < NOON(b)$, the occupation numbers of orbitals a and b being close to one for biradicals. For *meta*-benzyne at $R_{C1C3} = 205$ pm, this leads to $\chi = 19\%$. Alternatively, one may take directly twice the weight of the second configuration in the wave function, which amounts to 32% in this case.[40] For a more reliable (and structurally more complex) wave function, it is less obvious how to derive this quantity. Cremer analyzed the CCSD(T) wave function in terms of natural orbitals making reference to the benzene *NOON*s and found a biradical character of 20%.[6h] Given these small values and the quite substantial distance of the radical centers, the question arises how the coupling of the formally unpaired electrons takes place.

NBO Analysis. NBO analysis[13] as a qualitative scheme allows to analyze delocalizations in terms of basic orbital interactions. For single configuration wave functions, a donor−acceptor interaction between two (more or less localized) bonding and antibonding NBOs φ_i and φ_j* may be investigated by simple second-order perturbation theory (eq 1).[13]

$$E^{(2)}_{ij} = -2\frac{\langle\varphi_i|\hat{F}|\varphi_j^*\rangle^2}{\epsilon_j^* - \epsilon_i} \equiv -2\frac{F^2_{ij}}{\Delta\epsilon_{ij}} \qquad (1)$$

Table 4 shows some NBO occupancies, and the most important intramolecular donor−acceptor interactions are given within the NBO perturbative framework.

For both C1C3 separations investigated (160 and 210 pm), the most important delocalization is found to be the donation of electron density from the bonding C1C3 orbital into the C2H7 antibond, that is, a σ-allylic interaction similar to that proposed by Cramer and Debbert for *meta*-dehydropyridines, but stabilizing in the 2-electron case.[8a,b] Through-bond coupling involving the geminal C1C2 and C2C3 σ-bonds is of similar importance

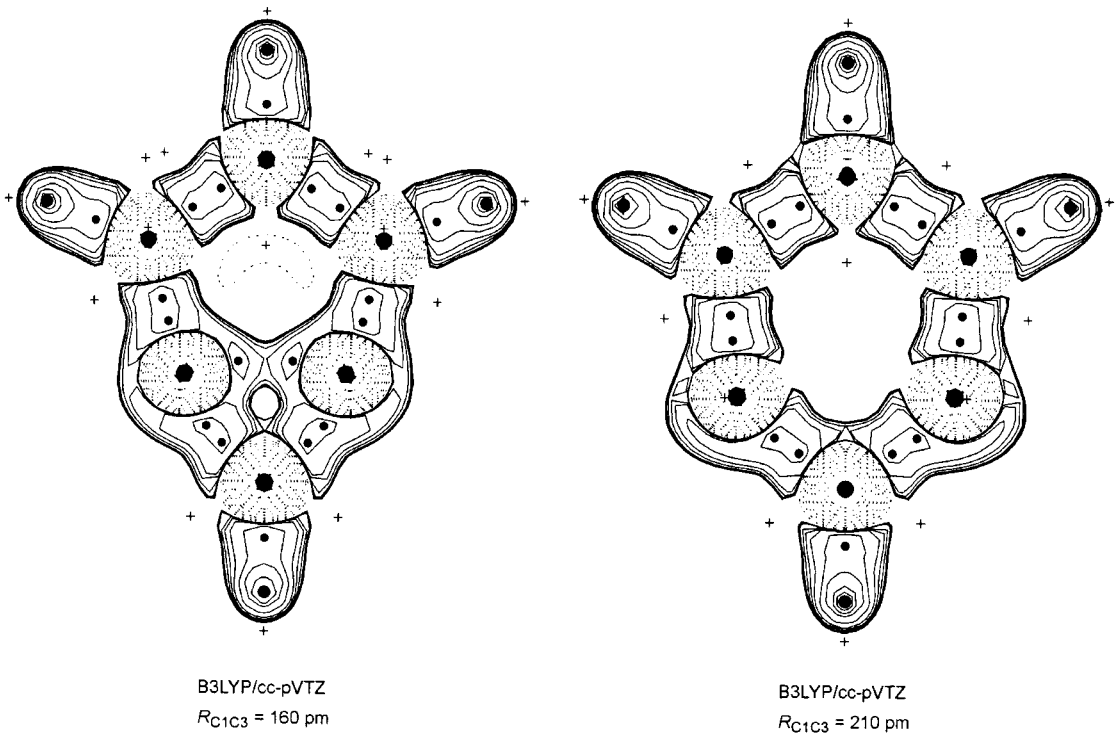

Figure 7. Contour maps of the Laplace concentrations $L(\mathbf{r}) = -\nabla^2\rho(\mathbf{r})$ of **1** for distances of $R_{C1C3} = 160$ pm and $R_{C1C3} = 210$ pm. Solid lines are in regions where electronic charge is concentrated ($L(\mathbf{r}) > 0$), dashed lines indicate charge depletion ($L(\mathbf{r}) < 0$). Maxima and minima in $L(\mathbf{r})$ are denoted by circles and crosses, respectively.

for larger distances between the radical centers but less important for bicyclic arrangements. It may, therefore, be possible to control spin coupling effectively by introducing substituents in the C2 position, but, of course, effects on the π-system have to be considered as well.[7a]

We conclude that neither description **1a** nor formula **1b** adequately describes *meta*-benzyne, and a formula like **1c** appears to give the most reasonable description.

1c

This view is nicely supported by the Laplace concentrations $L(\mathbf{r}) = -\nabla^2\rho(\mathbf{r})$ shown in Figure 7.

In regions where $\nabla^2\rho(\mathbf{r}) < 0$, charge is locally concentrated, whereas for $\nabla^2\rho(\mathbf{r}) > 0$, charge is locally depleted.[14] The extent of charge concentration and charge depletion are related via the local virial theorem (eq 2), which states that the potential-energy density $V(\mathbf{r})$ and the kinetic-energy density $G(\mathbf{r})$ add up at each point in space to the Laplace distribution.[14]

$$^1/_4\nabla^2\rho(\mathbf{r}) = 2G(\mathbf{r}) + V(\mathbf{r}) \tag{2}$$

Integration over the total molecular space must give the molecular virial theorem, and therefore the volume integral over the Laplacian vanishes:[14]

$$^1/_4 \int \nabla^2\rho(\mathbf{r})\mathrm{d}\mathbf{r} = 2\int G(\mathbf{r})\mathrm{d}\mathbf{r} + \int V(\mathbf{r})\mathrm{d}\mathbf{r} = 2T + V = 0 \tag{3}$$

This implies that fluctuations in the Laplace distribution summed over all space vanish. The same conclusion holds for an atomic basin, that is, a region of space bound by a zero flux surface S:[14]

$$\nabla\rho(\mathbf{r})\cdot\mathbf{n}(\mathbf{r}) = 0 \;\forall\; \mathbf{r} \in \mathbf{S} \tag{4}$$

Figure 7 reveals that for small separations ($R_{C1C3} = 160$ pm), two concentration lumps exist between the radical centers and therefore this structure is on the onset of chemical bond formation. For the more reliable structure ($R_{C1C3} = 210$ pm), the topology of the Laplace field shows that the description of C1C2C3 as a σ-allylic system and that the representation **1c** are intuitively appealing ways to describe the charge distribution within the *meta*-benzyne molecule.

5. Conclusions

meta-Benzyne is characterized by a very flat single-well potential-energy surface, and the equilibrium distance between the radical centers is 205 ± 5 pm. Coupling of the formally unpaired electrons occurs by through-space and through-bond interactions via the antibonding C2H7 and the geminal C1C2 and C2C3 bonds. The best representation of the electronic structure is a σ-allylic C1C2C3 system **1c**.

An accurate description of the *meta*-benzyne potential-energy surface requires a proper account for dynamic electron correlation. Near-degeneracy effects are important for larger C1C3 separations. Neither HF−SCF nor the hybrid functionals considered in this work are appropriate for the problem at hand. Pure GGA functionals, however, show a surprisingly good performance and especially BLYP gives a potential-energy surface that closely matches that obtained at high levels of wave function theory. The BLYP calculated vibrational spectrum is in excellent agreement with the one measured, and this functional also shows the best stability properties. It therefore seems to be the DFT method of choice for future work on *meta*-

benzynes. Our results clearly show that a bicyclic isomer **1b** does not exist and that the experimentally observed species has been correctly assigned to the monocyclic *meta*-benzyne structure.

Acknowledgment. This work was financially supported by the Deutsche Forschungsgemeinschaft and the Fonds der Chemischen Industrie. M.W. thanks the Fonds der Chemischen Industrie for a stipend. We thank Prof. Dr. Dieter Cremer, Göteborg University, for helpful hints and discussions.

Supporting Information Available: Energies of all calculated structures, Cartesian coordinates, and vibrational frequencies for many stationary points and a more detailed description of the NBO results are available as Supporting Information. This material is available free of charge via the Internet at http://pubs.acs.org.

References and Notes

(1) (a) Sander, W. *Acc. Chem. Res.* **1999**, *32*, 669. (b) Hoffman, R. W. *Dehydrobenzene and Cycloalkynes*; Academic Press: New York, 1967.

(2) (a) Wenk, H. H.; Sander, W. *Chem. Eur. J.* **2001**, *7*, 1837. (b) Wenk, H. H.; Balster, A.; Sander, W.; Hrovat, D. A.; Borden, W. T. *Angew. Chem., Int. Ed. Engl.* **2001**, *40*, 2295. (c) Sander, W.; Exner, M. *J. Chem. Soc., Perkin Trans. 2* **1999**, 2285. (d) Marquardt, R.; Balster, A.; Sander, W.; Kraka E.; Cremer, D.; Radziszewski, J. G. *Angew. Chem., Int. Ed. Engl.* **1998**, *37*, 955. (e) Sander, W.; Bucher, G.; Wandel, H.; Kraka, E.; Cremer, D.; Sheldrick, W. S. *J. Am. Chem. Soc.* **1997**, *119*, 10660. (f) Marquardt, R.; Sander, W.; Kraka E. *Angew. Chem., Int. Ed. Engl.* **1996**, *35*, 746. (g) Sander, W.; Marquardt, R.; Bucher, G.; Wandel, H. *Pure Appl. Chem.* **1996**, *68*, 353. (h) Bucher, G.; Sander, W.; Kraka, E.; Cremer, D. *Angew. Chem., Int. Ed. Engl.* **1992**, *35*, 746.

(3) (a) Thoen, K. K.; Kenttämaa H. I. *J. Am. Chem. Soc.* **1999**, *121*, 800. (b) Thoen, K. K.; Kenttämaa H. I. *J. Am. Chem. Soc.* **1997**, *119*, 3832.

(4) (a) Wenthold, P. G.; Squires, R. R.; Lineberger, W. C. *J. Am. Chem. Soc.* **1998**, *120*, 5279. (b) Wenthold, P. G.; Hu, J.; Squires, R. R. *J. Am. Chem. Soc.* **1996**, *118*, 11865. (c) Wenthold, P. G.; Squires, R. R. *J. Am. Chem. Soc.* **1994**, *116*, 6401.

(5) (a) Roth, W. R.; Hopf, H.; Horn, C. *Chem. Ber.* **1994**, *127*, 1765. (b) Zhang, X.; Chen, P. *J. Am. Chem. Soc.* **1992**, *114*, 3147. (c) Radziszewski, J. G.; Hess, B. A., Jr.; Zahradnik, R. *J. Am. Chem. Soc.* **1992**, *114*, 52. (d) Gronert, S.; DePuy, C. H. *J. Am. Chem. Soc.* **1989**, *111*, 9253. (e) Moini, M.; Leroi, G. E. *J. Phys. Chem.* **1986**, *90*, 4002.

(6) (a) Lindh, R.; Bernhardsson, A.; Schütz, M. *J. Phys. Chem. A* **1999**, *103*, 9913. (b) Cramer, C. J.; Nash, J. J.; Squires, R. R. *Chem. Phys. Lett.* **1997**, *277*, 311. (c) Kraka, E.; Cremer, D.; Bucher, G.; Wandel, H.; Sander, W. *Chem. Phys. Lett.* **1997**, *268*, 313. (d) Nash, J. J.; Squires, R. R. *J. Am. Chem. Soc.* **1996**, *118*, 11872. (e) Lindh, R.; Schütz, M. *Chem. Phys. Lett.* **1996**, *258*, 409. (f) Lindh, R.; Lee, T. J.; Bernhardsson, A.; Persson, B. J.; Karlström, G. *J. Am. Chem. Soc.* **1995**, *117*, 7186. (g) Lindh, R.; Persson, B. J. *J. Am. Chem. Soc.* **1994**, *116*, 4963. (h) Kraka, E.; Cremer, D. *J. Am. Chem. Soc.* **1994**, *116*, 4929. (i) Kraka, E.; Cremer, D. *Chem. Phys. Lett.* **1993**, *216*, 333. (j) Wierschke, W. S.; Nash, J. J.; Squires, R. R. *J. Am. Chem. Soc.* **1993**, *115*, 11958. (k) Nicolaides, A.; Borden, W. T. *J. Am. Chem. Soc.* **1993**, *115*, 11951.

(7) (a) Johnson, W. T. G.; Cramer, C. J. *J. Am. Chem. Soc.* **2001**, *123*, 923. (b) Cramer, C. J. *J. Chem. Soc., Perkin Trans. 2* **1999**, 2273. (c) Davico, G. E.; Schwartz, R. L.; Ramond, T. M.; Lineberger, W. C. *J. Am. Chem. Soc.* **1999**, *121*, 6047. (d) Langenaeker, W.; De Proft, F.; Geerlings, P. *J. Phys. Chem. A* **1998**, *102*, 5944.

(8) (a) Debbert, S. L.; Cramer, C. J. *Int. J. Mass Spectrom.* **2000**, *201*, 1. (b) Cramer, C. J.; Debbert, S. L. *Chem. Phys. Lett.* **1998**, *287*, 320. (c) Cramer, C. J. *J. Am. Chem. Soc.* **1998**, *120*, 6261. (d) Nam, H. H.; Leroi, G. E.; Harrison, J. F. *J. Phys. Chem.* **1991**, *95*, 6514.

(9) (a) Cramer, C. J.; Thompsom, J. *J. Phys. Chem. A* **2001**, *105*, 2091. (b) Kraka, E.; Cremer, D. *J. Am. Chem. Soc.* **2000**, *122*, 8245. (c) Koseki, S.; Fujimura, Y.; Hirama, M. *J. Phys. Chem. A* **1999**, *103*, 7672. (d) Schreiner, P. R. *Chem. Commun.* **1998**, 483. (e) Squires, R. R.; Cramer, C. J. *J. Phys. Chem. A* **1998**, *102*, 9072. (f) Schreiner, P. R. *J. Am. Chem. Soc.* **1998**, *120*, 4184. (g) Cramer, C. J.; Squires, R. R. *J. Phys. Chem. A* **1997**, *101*, 9191. (h) Ford, G. P.; Biel, E. R. *Tetrahedron Lett.* **1995**, *36*, 3663.

(10) (a) Washburn, W. N.; Zahler, R. *J. Am. Chem. Soc.* **1976**, *98*, 7827, 7828. (b) Washburn, W. N. *J. Am. Chem. Soc.* **1975**, *97*, 1615.

(11) Hess, B. A., Jr. *Eur. J. Org. Chem.* **2001**, 2185. In that work, a bicyclic structure **1b** of *meta*-benzyne is considered to be more probable than a monocyclic form **1a**. Since only B3LYP calculations have been carried out in that work, and this level of theory is clearly shown to be inadequate in the present paper, we do not agree with the conclusions of Hess.

(12) The finding that pure DFT works better for aromatic biradicals than hybrid methods was proposed by Schreiner et al. and Cramer et al. See, for example, ref 8c, 9f. For *para*-benzyne and the Bergman cyclization, the B3LYP functional gives better results than BLYP, especially when empirical correction schemes for spin contamination are applied: (a) Gräfenstein, J.; Hjerpe, A. M.; Kraka, E.; Cremer, D. *J. Phys. Chem. A* **2000**, *104*, 1748. See also 9b. A recent critical overview is found in (b) Jones, G. B.; Warner, P. M. *J. Am. Chem. Soc.* **2001**, *123*, 2134. Compare as well: (c) Chen, W.-C.; Chang, N.-Y.; Yu, C.-H. *J. Phys. Chem. A* **1998**, *102*, 2484. A more general comparison of different functionals can be found in (d) Koch, W.; Holthausen, M. C. *A Chemist's Guide to Density Functional Theory*; Wiley-VCH: Weinheim, 2000.

(13) Reed, A. E.; Curtiss, L. A.; Weinhold, F. *Chem. Rev.* **1988**, *88*, 899.

(14) (a) Popelier, P. *Atoms in Molecules*; Prentice Hall: Harlow, 2000. (b) Bader, R. W. F. *Chem. Rev.* **1991**, *91*, 893. (c) Bader, R. W. F. *Atoms in Molecules: A Quantum Theory*; Clarendon Press: Oxford, 1990. (d) Cremer, D.; Kraka, E. *Croat. Chem. Acta* **1984**, *57*, 1259. (e) Cremer, D.; Kraka, E. *Angew. Chem., Int. Ed. Engl.* **1984**, *23*, 627.

(15) (a) Seeger, R.; Pople, J. A. *J. Chem. Phys.* **1977**, *66*, 3045. (b) Bauernschmitt, R.; Ahlrichs, R. *J. Chem. Phys.* **1996**, *104*, 9047. See also: (c) Davidson, E. R. *Int. J. Quantum Chem.* **1998**, *69*, 241. (d) Perdew, J. P.; Savin, A.; Burke, K. *Phys. Rev. A* **1995**, *51*, 4531.

(16) (a) Woon, D. E.; Dunning, T. H. *J. Chem. Phys.* **1993**, *98*, 1358. (b) Kendall, R. A.; Dunning, T. H.; Harrison, R. J. *J. Chem. Phys.* **1992**, *96*, 6796. (c) Dunning, T. H. *J. Chem. Phys.* **1989**, *90*, 1007.

(17) Becke, A. D. *Phys. Rev. A* **1988**, *38*, 3098.

(18) (a) Burke, K.; Perdew, J. P.; Wang, Y. In *Electronic Density Functional Theory: Recent Progress and New Directions*; Dobson, J. F., Vignale, G., Das, M. P., Eds.; Plenum: New York, 1998. (b) Perdew, J. P.; Chevary, J. A.; Vosko, S. H.; Jackson, K. A.; Pederson, M. R.; Singh, D. J.; Fiolhais, C. *Phys. Rev. B* **1993**, *48*, 4978. (c) Perdew, J. P.; Burke, K.; Wang, Y. *Phys. Rev. B* **1996**, *54*, 16533.

(19) Lee, C.; Yang, W.; Parr, R. G. *Phys. Rev. B* **1988**, *37*, 785.

(20) Perdew, J. P.; Ernzerhof, M.; Zupan, A.; Burke, K. *J. Chem. Phys.* **1998**, *108*, 1522.

(21) (a) Becke, A. D. *J. Chem. Phys.* **1993**, *98*, 5648. Compare also: (b) Stevens, P. J.; Devlin, F. J.; Chablowski, C. F.; Frisch, M. J. *J. Phys. Chem.* **1994**, *98*, 11623.

(22) Frisch, M. J.; Trucks, G. W.; Schlegel, H. B.; Scuseria, G. E.; Robb, M. A.; Cheeseman, J. R.; Zakrzewski, V. G.; Montgomery, J. A., Jr.; Stratmann, R. E.; Burant, J. C.; Dapprich, S.; Millam, J. M.; Daniels, A. D.; Kudin, K. N.; Strain, M. C.; Farkas, O.; Tomasi, J.; Barone, V.; Cossi, M.; Cammi, R.; Mennucci, B.; Pomelli, C.; Adamo, C.; Clifford, S.; Ochterski, J.; Petersson, G. A.; Ayala, P. Y.; Cui, Q.; Morokuma, K.; Malick, D. K.; Rabuck, A. D.; Raghavachari, K.; Foresman, J. B.; Cioslowski, J.; Ortiz, J. V.; Stefanov, B. B.; Liu, G.; Liashenko, A.; Piskorz, P.; Komaromi, I.; Gomperts, R.; Martin, R. L.; Fox, D. J.; Keith, T.; Al-Laham, M. A.; Peng, C. Y.; Nanayakkara, A.; Gonzalez, C.; Challacombe, M.; Gill, P. M. W.; Johnson, B. G.; Chen, W.; Wong, M. W.; Andres, J. L.; Head-Gordon, M.; Replogle, E. S.; Pople, J. A. *Gaussian 98*, Gaussian, Inc.: Pittsburgh, PA, 1998.

(23) Roos, B. O.; Taylor, P. R.; Siegbahn, P. E. M. *Chem. Phys.* **1980**, *48*, 157.

(24) Hampel, C.; Peterson, K.; Werner, H.-J. *Chem. Phys. Lett.* **1992**, *190*, 1.

(25) (a) Stanton, J. F.; Gauss, J.; Bartlett, R. J. *J. Chem. Phys.* **1992**, *97*, 5554. (b) Lee, T. J.; Kobayashi, R.; Handy, N. C.; Amos, R. D. *J. Chem. Phys.* **1992**, *96*, 8931. (c) Kobayashi, R.; Handy, N. C.; Amos, R. D.; Trucks, G. W.; Frisch, M. J.; Pople, J. A. *J. Chem. Phys.* **1991**, *95*, 6723. (d) Handy, N.; Pople, J. A.; Head-Gordon, M.; Raghavachari, K.; Trucks, G. W. *Chem. Phys. Lett.* **1989**, *164*, 185.

(26) Brueckner, K. A. *Phys. Rev.* **1954**, *96*, 508.

(27) Stanton, J. F. *Chem. Phys. Lett.* **1997**, *281*, 130.

(28) (a) Lee, T. J.; Scuseria, G. E. In *Quantum Mechanical Electronic Structure Calculations with Chemical Accuracy*; Langhoff, S. R. Ed.; Kluwer Academic Publishers: Dordrecht, 1997. (b) Bartlett, R. J. In *Modern Electronic Structure Theory*; Yarkony, D. R. Ed.; World Scientific: Singapore, 1995. (c) Taylor, P. R. In *Lecture Notes in Quantum Chemistry*; Roos, B. O., Ed.; Springer: Berlin, 1994. (d) Scuseria, G. E.; Lee, T. J. *J. Chem. Phys.* **1990**, *93*, 5851. (e) Raghavachari, K.; Trucks, G. W.; Pople, J. A.; Head-Gordon, M. *Chem. Phys. Lett.* **1989**, *157*, 479. (f) Purvis, G. D.; Bartlett, R. J. *J. Chem. Phys.* **1982**, *76*, 1910.

(29) Lee, T. J.; Taylor, P. R. *Int. J. Quantum Chem.* **1989**, *S23*, 199.

(30) A nice review concerning calculations on open-shell molecules, which contains some remarks on singlet biradicals, has been written by Bally, T.; Borden, W. T. In *Reviews in Computational Chemistry*; Boyd, D. B., Lipkowitz, K. B., Eds.; Wiley-VCH: New York, 1999; Vol. 13.

(31) (a) Werner, H.-J.; Knowles, P. J. *J. Chem. Phys.* **1988**, *89*, 5803. (b) Knowles, P. J.; Werner, H.-J. *Chem. Phys. Lett.* **1988**, *145*, 514.

(32) Davidson, E. R. In *The World of Quantum Chemistry*; Daudel, R., Pullman, B., Eds.; Reidel: Dordrecht, 1974.

(33) (a) Andersson, K.; Roos, B. O. In *Modern Electronic Structure Theory*; Yarkony, D. R. Ed.; World Scientific: Singapore, 1995. (b) Andersson, K.; Roos, B. O. *Int. J. Quantum Chem.* **1993**, *45*, 591. (c) Werner, H.-J. *Mol. Phys.* **1996**, *89*, 645.

(34) Werner, H.-J.; Knowles, P. J. *Molpro 2000.1*; Birmingham, 1999.

(35) Biegler-König, F.; Schönbohm, J.; Bayles, D. *J. Comput. Chem.* **2001**, *22*, 545.

(36) Carsky, P.; Hubak, E. *Theor. Chim. Acta* **1991**, *80*, 407. Compare also ref 30.

(37) For recent work, see: (a) Dunning, J. H., Jr. *J. Phys. Chem. A* **2000**, *104*, 9062. (b) Dunning, J. H., Jr.; Peterson, K. A. *J. Chem. Phys.* **2000**, *113*, 7799. (c) Petersson, G. A.; Frisch, M. J. *J. Phys. Chem. A* **2000**, *104*, 2183 and references therein. (d) Martin, J. M. L. In *Density Functional Theory*; Geerlings, P., De Proft, F., Langenaeker, W., Eds.; VUBPRESS: Brussels, 1999. (e) Fast, P. L.; Sanchez, M. L.; Truhlar, D. G. *J. Chem. Phys.* **1999**, *111*, 2921. (f) Truhlar, D. G. *Chem. Phys. Lett.* **1998**, *294*, 45. (g) Martin, J. M. L. *Chem. Phys. Lett.* **1996**, *259*, 669. Compare also: (h) Csaszar, A. G.; Allen, W. D.; Schaefer III, H. F. *J. Chem Phys.* **1998**, *108*, 9751.

(38) (a) Schwartz, C. In *Methods in Computational Physics*; Alder, B. J. Ed.; Academic Press: New York, 1963. Compare also: (b) Kutzelnigg, W. *Theor. Chim. Acta* **1985**, *68*, 445. (c) Kutzelnigg, W.; Morgan III, J. D. *J. Chem. Phys.* **1992**, 96, 4484. (d) Kutzelnigg, W.; Morgan III, J. D. *J. Chem. Phys.* **1992**, *97*, 8821.

(39) Döhnert, D.; Koutecky, J. *J. Am. Chem. Soc.* **1980**, *102*, 1789.

(40) Schmidt, M. W.; Gordon, M. S. *Annu. Rev. Phys. Chem.* **1998**, *49*, 233.